

# Mixture Fraction Measurements During The Hot-Jet Ignition Of Hydrogen/Air Mixtures

R. Sadanandan<sup>1\*</sup>, D. Markus<sup>1</sup>, R. Schießl<sup>2</sup> and U. Maas<sup>2</sup>

<sup>1</sup>Physikalisch Technische Bundesanstalt, Braunschweig, Germany.

<sup>2</sup>Institute of Technical Thermodynamics, University of Karlsruhe, Germany.

## Abstract

Instantaneous, quantitative, two-dimensional, spatially resolved mixture fraction maps in a re-igniting hot jet configuration in a H<sub>2</sub>/air system are measured. The measurement is based on a combination of laser-induced fluorescence (LIF) of seeded NO and detailed numerical simulations. From a large set of computed scenarios in a jet/fuel-air mixture configuration, correlations between NO-LIF signals and mixture fraction, valid in a range of lower temperatures (< approx. 1300K) before the onset of combustion, are deduced by spectroscopical simulations. These correlations are used to convert planar NO LIF-images, measured in an experimental hot-jet ignition setup, into quantitative mixture fraction maps. We give examples for measurements, and discuss potentials and limitations of our approach.

## Introduction

The ignition of combustible mixtures by hot free jets is an important issue in a variety of fields like combustion engines [1], nuclear safety [2], propulsion systems [3]. Information regarding the fundamental mechanisms behind the hot turbulent jet ignition process is vital in the field of explosion protection not only for preventing accidental damages of catastrophic dimensions, but also for assisting manufacturers in the designing of preventive equipments.

Some of the earliest known works on the ignition of explosive mixtures by hot gas are from Wolfhard [4] where the ignition problem was studied by continuous injection of hot gas onto a cold explosive mixture. The studies revealed that the hot gas ignition temperatures bear little relation to the spontaneous ignition temperatures. Similar works from Meyer et al. [5], Philips [6] and Moen et al. [7] later on also showed the importance of gas dynamic properties of the jet on the ignition process. Investigation on the chemical kinetics of H<sub>2</sub>/O<sub>2</sub> systems by Blouch et al. [8] in turbulent counterflow configuration of heated air and cold hydrogen/nitrogen jets shows that the ignition temperature of hydrogen increases with turbulence and pressure. However, studies using direct numerical simulations (DNS) on the autoignition of a hydrogen-air scalar mixing layer in homogeneous turbulence [9] divulge that the ignition delays appear to be quite insensitive to the turbulence intensity, because, as ignition is a local event, there will always be some well-mixed regions as long as some turbulence exists.

Laser diagnostics has become an integral part of turbulent combustion research, owing to its remote and non-intrusive nature [10]. Different experimental approaches have been employed to obtain instantaneous multidimensional measurements of mixture fraction. Laser induced fluorescence (LIF) draws special

attention in view of its high sensitivity and species specificity with high spatial and temporal resolution [11]. Mixture fraction studies using LIF of NO as tracers are particularly attractive as NO has good thermal stability, a well-characterized spectroscopy and because it provides high SNR values due to its excellent fluorescence characteristics [12]. To infer quantitative mixture fractions, however, is problematic due to the complex dependency between the LIF-signal and mixture fraction.

In this work, we approach this problem by systematically combining NO LIF-measurements with detailed numerical simulations of the underlying physical and chemical processes, and with spectroscopical simulations of the NO LIF-signal as a function of the state variables (species concentrations, temperature). By numerically studying a set of scenarios in the jet-fuel/air mixture configuration, we can infer a representative set of state vectors (state variables temperature, species mass fractions). By calculating the LIF-signals corresponding to these state vectors, we find correlations between the LIF-signals and NO mass fractions. These correlations describe a dependence of the LIF-signal on the mixture fraction, which is valid for the conditions covered by the underlying set of numerical simulations.

For certain conditions ( $T < \text{ca. } 1300\text{K}$ , spatially uniform pressure), we find sharp LIF- $\xi$  correlations. By exploiting these correlations, two-dimensional and spatially resolved NO mass fraction fields can be inferred from measured planar LIF-signals. From NO mass fraction fields, mixture fraction fields can be calculated.

Due to the lack of similar sharp correlations for higher temperatures, application of the method is limited to times before ignition and shortly after ignition, before the combustion-induced temperature increase makes a quantification of LIF-signals more difficult.

This paper is structured as follows. The method used for the quantitative measurement of mixture fraction involves both numerical calculations and experimental diagnostics. These two sections are

---

\*Corresponding author: [Rajesh.Sadanandan@ptb.de](mailto:Rajesh.Sadanandan@ptb.de)  
Proceedings of the European Combustion Meeting  
2005

briefly explained in the methodology section. It is followed by an overview of the experimental set-up and the results sections, where the major results are shown along with a discussion.

### Theoretical Background

When the hot jet enters a cool, unburned fuel/air mixture, this mixture can ignite due to the hot temperatures occurring during the mixing process. Neither the hot jet nor the unburned mixture alone can undergo ignition; mixing is required in order to provide both high temperatures (from the hot jet) and a fuel/air mixture (from the unburned gas). To describe this mixing process, the mixture fraction  $\xi$ , defined as the mass fraction of all atoms originating from the hot jet, is used. The gradient of a mixture fraction field is related to the local instantaneous mixing speed (scalar dissipation rate) between jet ( $\xi = 1$ ) and fuel/air mixture ( $\xi = 0$ ). This, in turn, is a measure for the local interaction of physical processes with chemical reactions and is therefore a key for the understanding of the re-ignition process.

To observe mixture fraction fields in an experiment, using a LIF-technique seems to be appropriate due to the high temporal and spatial resolution that LIF can provide. An often found problem in LIF measurements, however, is the transformation of signal strengths into quantitative values of the desired state variable (e.g., species concentrations or mixture fractions). One principal reason for this difficulty is that the LIF-signal is a function of several state variables (temperature, concentrations of the species acting as LIF-quenchers), and not of desired state variable alone.

One way of solving this problem is to use additional information from numerical simulations. This information is used to ascertain if correlations between the desired quantities and the measured LIF-signal exist. In general, the measured signal intensity  $S$  emitted from a small volume can be written as a function of the state variables (pressure, temperature, species concentrations) and experimental parameters (e.g., intensity of the laser beam or sheet used for LIF-excitation, efficiency of the employed detector, or the transmission of the used optical line):  $S = f(p, T, c_i, \alpha)$ , where  $\alpha$  represents the experimental parameters (like the ones mentioned above).

For the special case of a LIF experiment in the linear regime of fluorescence, this function reads

$$S = I_{\text{LIF}} \propto I_{\text{laser}} N_{\text{NO}} f_{\text{B}}(T) \sigma_{\text{eff}} \frac{A_{21}}{A_{21} + Q_{21}(T, p, x_i)} \quad (1)$$

with the incident laser intensity  $I_{\text{laser}}$ , the total number density of NO molecules  $N_{\text{NO}}$ , the Boltzmann fraction of molecules in the laser-excited ground state  $f_{\text{B}}$ , the effective absorption cross-section  $\sigma_{\text{eff}}$ , the Einstein coefficient  $A_{21}$  for spontaneous emission and  $Q_{21}$  the quenching rate. Therefore the LIF-intensity is a function of pressure  $p$ , temperature  $T$  and the mole frac-

tion  $x_i$  of all species  $i$  ( $i=1, \dots, n_s$ , where  $n_s$  is the number of species).

Mathematically, (1) is one equation of multiple unknowns (e.g.,  $T, x_i$ ). The purpose of a quantitative measurement is to deduce the value of a state variable from the measurement signal  $S$ , i.e., to solve eq. (1) for the desired state variable. Since the number of species for a hydrogen/air combustion system is at least  $n_s=9$ , eq. (1) is strongly underdetermined in our case, and it is, in general, not possible to obtain a state variable from (1). One way to solve this problem is to use additional information, e.g., from other experiments or from numerical simulations.

### Methodology

#### Numerical Procedure

A large set of state vectors for different scenarios, representing the interaction of hot burnt gas with unburnt hydrogen air mixture, were calculated using a one-dimensional approach. Details of the setup of these simulations are given in [13]. The domain of flow velocities and initial conditions used for the simulations were taken from previous experimental [14] and numerical work [15]. The chemical reaction mechanism included NO formation, in order to account for nascent NO that possibly interferes with the seeded NO during measurements. Gasdynamic effects (pressure waves or shock waves) were not included in the calculations.

For each of the computed scenarios, the corresponding NO-LIF signals are computed according to equation (1), using the program LIFSim [16]. According to equation (1), the computations use a detailed description of the spectroscopy, including quenching, spectral line broadening and shifting and changes in Boltzmann fraction with temperature. The information obtained in this way is used for selecting an excitation scheme that delivers a sharp correlation between the computed NO-LIF signal and NO mass fraction. These correlations are used to convert the measured NO-LIF signals into NO-mass fraction values  $w_{\text{NO}}$ . From these, the mixture fraction  $\xi$  is calculated using the formula

$$\xi = \frac{w_{\text{NO}} - w_{\text{NO,c}}}{w_{\text{NO,h}} - w_{\text{NO,c}}} \quad (2)$$

where the subscript ‘c’ refers to the unburned mixture and the subscript ‘h’ refers to the hot jet. This formula assumes that the influence of differential diffusion can be neglected in the investigated system.

For the present experiments, the measurements were restricted to pre-ignition times as the aim was to understand the events leading to ignition of explosive mixtures by hot turbulent jets. So the basic criteria were to find an excitation scheme which features a sharp correlation between NO-LIF and NO mass fraction for low temperature ranges (600 – 1200 K) corresponding to pre-ignition times. Based on the computational results obtained, the excitation line

$Q_1(23.5)$  was selected for mixture fraction measurements.

Figure 1 shows the variation of the theoretical LIF-signal  $S_{\text{theo}}$  ( $S_{\text{theo}} = I_{\text{LIF}}$  from formula (1)) with NO mass fraction. As initial conditions for the numerical calculations, the temperature of the hot jet  $T_b$  was varied between 1100 K and 1300 K.

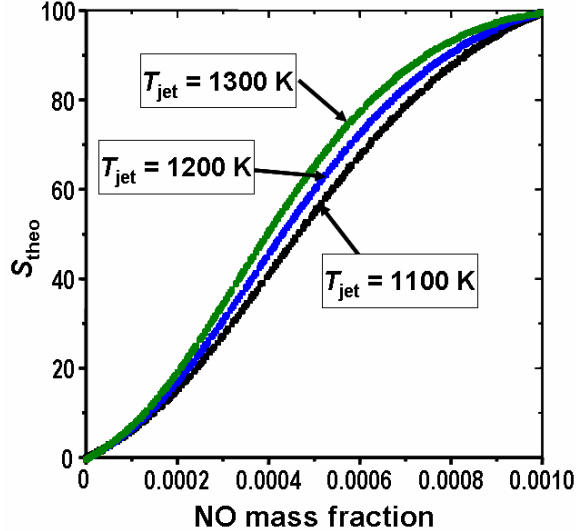


**Figure 1:** Variation of the theoretical LIF signal  $S_{\text{theo}}$  with NO mass fraction, calculated from a set of jet-fuel/air interaction simulations (jet exit temperatures  $T=1100\text{K}$ ,  $T=1200\text{K}$ ,  $T=1300\text{K}$ ) using detailed transport and chemistry. For the graphical representation,  $S_{\text{theo}}$  is shown normalized here.

These values were selected based on the results of earlier Rayleigh and Schlieren measurements [14] that were performed with the same experimental setup. Using a range of initial conditions allowed to study the sensitivity of the correlations with respect to these initial conditions. The chemical composition of the hot-jet gas was assumed to be in chemical equilibrium at the respective burned gas temperature. It can be seen (figure 1b) that even for a burnt gas temperature change of  $\pm 100\text{K}$  around 1100K, the unsharpness in the correlation is minimal and within an acceptable range. Note for the graphical representation, the signals  $S_{\text{theo}}$  are shown normalized.

### Experimental set-up

An optically accessible, constant volume combustion cell as shown in figure 2 was used for the experiments. The cell consists of two chambers with a constant diameter nozzle connecting the chambers. The cylindrical smaller chamber is 80 mm in length and 60 mm in diameter, rendering to a volume of 0.226 litres. The second chamber, with three quartz windows for optical access, has a volume of 12 litres. Both chambers were filled with a 28% hydrogen/air mixture (vol./vol.) at the beginning of the experiments.

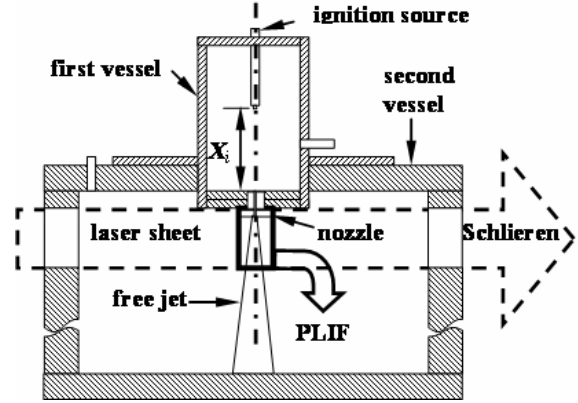


**Figure 2:** Schematic of the combustion cell

The hydrogen/air mixture in the first vessel was ignited by means of electrical discharges on the symmetrical axis of the vessel at a distance  $X_i$ . The pressure ratio across the nozzle  $p_1/p_2$  was varied by changing the value of  $X_i$ . The hot burned gas from the first chamber expanded through the nozzle and impinged into the stagnant unburned hydrogen/air mixture in the second chamber, possibly initiating ignition and combustion. Experiments were repeated with a combination of different pressure ratios and nozzle diameters in order to investigate the influence of jet velocities on the mixing and ignition process. Laser Schlieren imaging was employed to study the spatial and temporal development of the turbulent jet, along with NO-PLIF imaging for mixture fraction studies. The optical arrangement used for the measurements is shown in figure 3. It consisted of a Nd:YAG –dye laser combination for the NO-LIF experiments and a He-Ne (20 mW @ 632.8 nm) laser for the laser Schlieren experiments. The frequency tripled (355 nm) output from the Nd:YAG laser was used to pump the dye laser (linewidth 0.002 nm) operating on Coumarin 120 dye. The excitation laser pulses for the LIF measurements were obtained by frequency doubling the dye laser output. For NO-LIF the laser was tuned to the  $Q_1(23.5)$  transition at 225.49 nm in the  $\nu''=0$ ,  $\nu'=0$  of the  $A^2\Sigma^+-X^2\Pi$  system. Subsequent LIF fluorescence in the A-X (0,1)-(0,5) bands was observed using a UG5 filter which also blocked direct laser scattering and the Rayleigh signal at 226 nm. Cylindrical lenses were used to convert the laser beam into a sheet of approximately 20 mm in height and 300  $\mu\text{m}$  in thickness. A small portion of the laser sheet was split off and focused into a cell containing a diluted solution of fluorescent dye. The raw LIF images were corrected for shot-to-shot laser sheet profile variations using this cell fluorescence profile, which was imaged on to the side of the same CCD as used for NO-LIF.

The detection system consisted of two ICCD cameras, a Flame Star high speed ICCD camera (La Vision, 12 bit, 384 x 288 pixel array) coupled to a UV lens (Halle, 100 mm, f/2) for the LIF visualization and a Streak Star high speed ICCD camera (LaVision, 14 bit dynamic resolution, 384 x 576 pixel

array) coupled to a Sigma zoom lens (75-300 mm, 4-5.6 f) for Schlieren experiments. The imaged region was  $38.3 \times 28.5$  mm and  $38 \times 39$  mm for the LIF and Schlieren images, respectively. The CCD array was gated to yield an exposure time of 200 ns to capture the NO-fluorescence. The time gap between the four Schlieren frames was  $50 \mu\text{s}$  with an exposure time of  $1 \mu\text{s}$  each. The timing between the laser pulses and different camera gate openings was synchronised by means of a delay generator circuit.

### Results and Discussion

Variations in the pressure ratio  $p_1/p_2$  (see above) lead to a change in jet velocities, thereby possibly largely altering the initial conditions of the jet ( $T_b$ , and therefore also the composition, and  $v_b$ ). Only some representative results are shown here.

The 2D mixture fraction images deduced from the NO-LIF images for  $p_1/p_2 = 1.44$  and  $d = 0.8$  mm are shown in figure 4b. The abrupt stop in the lower half is not genuine, but is due to the finite height of the laser sheet. The visible fluorescence is from *seeded* NO only; this follows from experiments that were performed in the same way, but without NO seeding. In those experiments, no LIF signal was observed, therefore no detectable amounts of NO can have been formed in the flame in chamber 1.

At  $p_1/p_2 = 1.44$  and  $d = 0.8$  mm, the burnt gases failed to ignite the fuel/air mixture in the second

chamber. This justifies the application of the computed NO-LIF- $\xi$  correlations, and they were used to transform the measured LIF-images into the shown mixture fraction fields. Figure 4a shows a sequence of Schlieren images corresponding to each mixture fraction image with respect to time. The Schlieren images serve to provide complementary information, namely the overall geometry of the jet and the presence of high-temperature regions, making it easier to ascertain the validity of the underlying assumptions for mixture fraction measurements. Figure 5 shows the axial and lateral mixture fraction profiles deduced from the mixture fraction images. The analysis starts at a point approximately 1.5 mm away from the nozzle exit ( $X=0$ ), in order to avoid influence of laser light scattered from the nozzle.

Figure 6 shows images of a quantity derived from LIF images according to the correlation shown above (this is *not* the mixture fraction in this case, since here the correlation derived above is not valid), and Schlieren images for a case of ignition of fuel/air mixture by the hot burnt gases. The images correspond to  $p_1/p_2 = 1.31$  and  $d = 1.0$  mm. The pressure waves produced by the impact of the burnt gases on the unburnt gases create a density gradient ahead of the jet, as can be seen in the first Schlieren image. The Schlieren sequences also indicate that re-ignition occurs between  $t = 1960 \mu\text{s}$  and  $2010 \mu\text{s}$ .

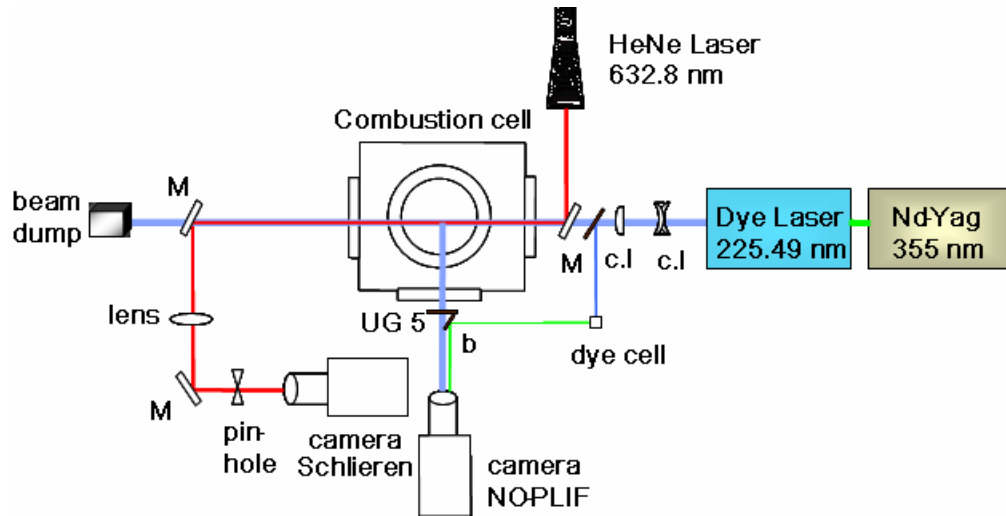


**Figure 3:** Schematic of the optical configuration; c.l.: cylindrical lens, M: mirror, b: beam splitter

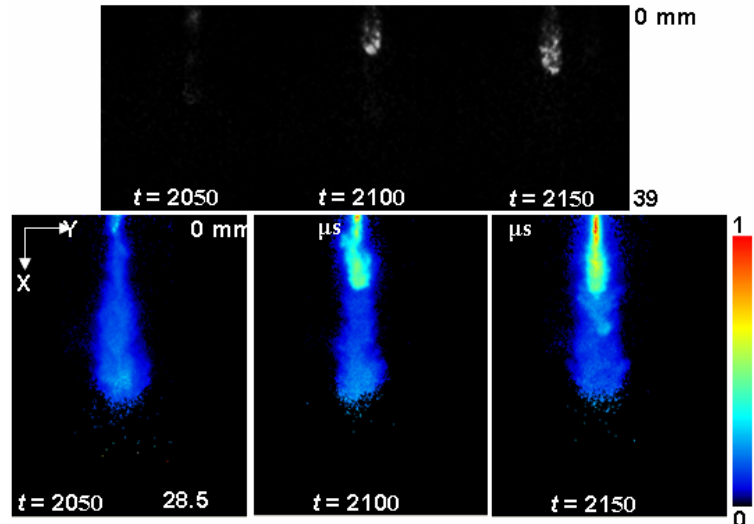


**Figure 4:** (a) Laser Schlieren sequences and (b) mixture fraction images for  $p_1/p_2 = 1.44$  and  $d = 0.8$  mm;  $t$  refers to the time after ignition in the first chamber and 0 mm refers to 1.5 mm after nozzle exit. Times are given in microseconds.

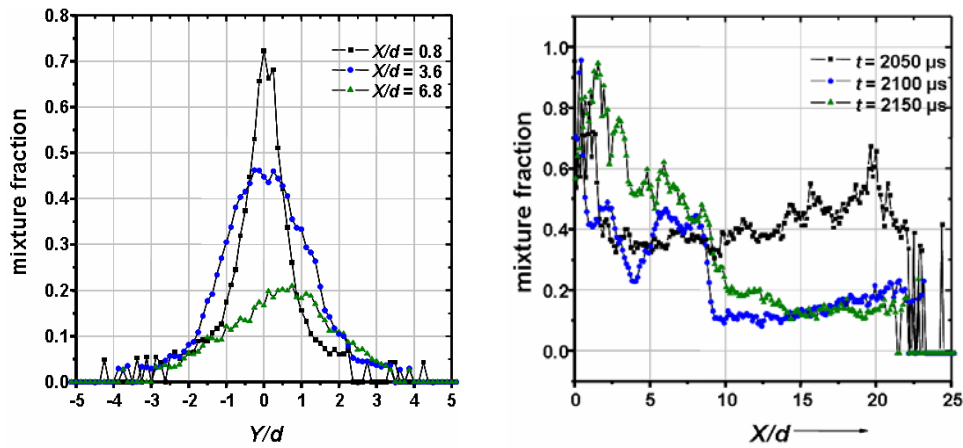


**Figure 5:** Axial mixture fraction profiles at different nozzle distances and lateral mixture fraction profiles at  $t = 2050 \mu\text{s} \dots 2150 \mu\text{s}$  for the images in fig. 4.

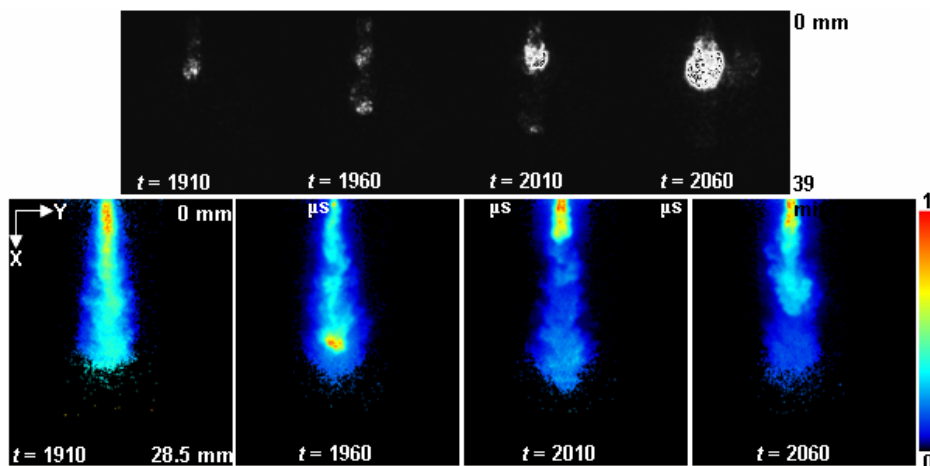


**Figure 6:** Laser Schlieren sequences (top) and images derived from LIF-images using the correlations shown in fig. 1 (bottom), for  $p_1/p_2 = 1.31$  and  $d = 1.0$  mm. Note that in this case, the images on the bottom do *not* represent mixture fraction, since the correlation is not valid in this situation (see discussion in the text). Times are given in microseconds.

As outlined above, the correlation used here is sharp at low temperatures, corresponding to pre-ignition times ( $t = 1910 \mu\text{s}$ ). It is not valid in cases where gasdynamic effects are present, as seen, e.g., at  $t = 1960 \mu\text{s}$ . Using the correlations as a basis for measurements in these cases is wrong and can lead to unphysical values of mixture fraction (e.g., values greater than 1). Likewise, the sharp drop in the mixture fraction values, seen in high temperature regions associated with combustion after re-ignition ( $t = 2010 \mu\text{s}$  and  $2060 \mu\text{s}$ ), is most likely not genuine. No reliable information about mixture fraction can be inferred from the images in this case.

### Conclusions

Quantitative, instantaneous and two dimensional mixture fraction images during the ignition of hydrogen/air mixtures by hot burnt gases are obtained using a combination of experiment (planar LIF of seeded NO) and numerical analysis. The numerical analysis is used to establish the scenarios (combinations of state variables like temperature and species concentrations) that are representative for the investigated system. By calculating the theoretical LIF-signal for this representative set of state variables, correlations between LIF-signals and NO mass fractions are found.

In cases where ignition and subsequent combustion have not yet raised the temperature to too high values (larger than ca. 1300K), we can use the correlations to infer 2D mixture fraction fields from LIF-measurements. The accuracy of the results depends on the "sharpness" of the correlations. If the initial conditions of the investigated system (in our case, especially the temperature) are not known exactly, the dependence of the correlations on the initial conditions has to be assessed by parametric studies. In our case, these uncertainties were found to have a minor influence on the correlations.

The results also highlight the limitations of the correlation used. If scenarios occur that have not been covered by the numerical simulations, applying the computed correlations for measurements is invalid. This is clearly true for cases involving gas dynamic effects and high temperatures. This calls for measurements using an alternative excitation line or a simultaneous, second measurement strategy to treat those cases.

### Acknowledgements

The authors are grateful to Wolfgang Bessler (Interdisziplinäres Zentrum für Wissenschaftliches Rechnen, University of Heidelberg), and Christof Schulz (Institut für Verbrennung und Gasdynamik, University of Duisburg) for their program LIFSIM for the calculation of NO-LIF signals.

### References

- [1] E. Murase, S. Ono, K. Hanada, A.K. Oppenheim, *Combustion Science and Technology* 113, 167-177 (1996).
- [2] N. Djebaili, R. Lisbet, G. Dupre, C. Paillard, *Proc. Comb. Inst.* 25, 1539-1545 (1994).
- [3] D.H. Lieberman, K.L. Parkin, J.E. Shepherd, *AIAA paper* 02-3909 (2002).
- [4] H.G. Wolfhard, *Jet Propulsion* 12 798-804 (1958).
- [5] J.W. Meyer, P.A. Urtiew, A.K. Oppenheim, *Combust. Flame* 14 13-20 (1970).
- [6] H. Phillips, *Combust. Flame* 19, 187-195 (1972).
- [7] I.O. Moen, D. Bjerketvedt, A. Jenssen, P.A. Thibault, *Combust. Flame* 61 285-291 (1985).
- [8] J.D. Blouch, C.K. Law, *Combust. Flame* 132, 512-522 (2003).
- [9] H.G. Im, J.H. Chen, C.K. Law, *Proc. Comb. Inst.* 27, 1047-1056 (1998).
- [10] J. Wolfrum, *Proc. Comb. Inst.* 27, 1-41 (1998).
- [11] R.K. Hanson, *Proc. Comb. Inst.* 21, 1677-1691 (1987).
- [12] J.A. Sutton, J.F. Driscoll, *Proc. Comb. Inst.* 29, 2727-2734 (2002).
- [13] U. Maas, J. Warnatz, *Combust. Flame* 74, 53-69 (1988).
- [14] M. Beyer, *Fortschrittsberichte VDI, Reihe 21, Nr. 228* (1997).
- [15] D. Markus, PhD Thesis, University of Stuttgart (2002).
- [16] W.G. Bessler, C. Schulz, V. Sick, J.W. Daily, *Joint meeting of the US sections of the Combustion Institute* (2003) D33 1-6.
- [17] R. Sadanandan, D. Markus, M. Spilling, R. Schiessl, U. Maas, J. Olofsson, H. Seyfried, M. Richter, M. Alden, *11th International Symposium on Loss Prevention and Safety Promotion in the Process Industries* (2004) 3245-3252.